Optimal Aperture Sizing to Minimize Power and Mode Mismatch Losses in Gaussian Beam Propagation

ELEONORA POLINI[1,3,*], ROMAIN BONNAND [1], MARTINA DE LAURENTIS [2] AND EDWIGE TOURNEFIER[1]

[1] *Laboratoire d'Annecy de Physique des Particules (LAPP), Univ. Grenoble Alpes, Université Savoie Mont Blanc, CNRS/IN2P3, 233F-74941 Annecy, France*
[2] *Department of Physics, University of Napoli "Federico II", Italy and INFN Napoli*
[3] *Now at Université Côte d'Azur, Observatoire de la Côte d'Azur, CNRS, Artemis, F-06304 Nice, France*
[*] *eleonora.polini@oca.eu*

Abstract:

Losses in optical experiments are critical and arise from various sources and require careful identification, analysis, and mitigation. This paper focuses on Gaussian beam propagation through circular apertures, examining both optical and mode mismatch losses. Traditional rules for aperture size become insufficient at precision levels below 1 ppm, necessitating a more detailed analysis, including lateral misalignment effects. By refining aperture selection criteria, this work enhances prior studies to meet modern experimental constraints. These results are particularly relevant for large-scale optical systems, such as gravitational wave detectors, where minimizing losses is essential for achieving the required sensitivity and performance.

1. Introduction

In many optical experiments, Gaussian beams propagate through optical elements with apertures, such as diaphragms and baffles. These elements are often used to block secondary beams while allowing the main beam to pass through their aperture.

The transmitted Gaussian beam experiences both power and mode mismatch losses. Depending on the experimental constraints, these losses must remain below a given threshold. In the following, we analyze all possible mechanisms of Gaussian beam degradation and provide a practical criterion to select the appropriate aperture size based on the requirements of the experiment.

We recall that the transverse intensity profile of a Gaussian beam with power P can be described by the function:

$$I(r,z) = \frac{2P}{\pi w(z)^2} e^{-2\frac{r^2}{w(z)^2}} \tag{1}$$

where $w(z)$ is the beam radius and r is the radial coordinate in a plane perpendicular to the propagation direction z. As a consequence, the power of a Gaussian beam passing through a circular aperture is not fully transmitted.

For example, a hard aperture with radius $a = w(z)$ transmits approximately 86.5% of the optical power. Increasing the aperture radius to $1.5w(z)$ or $2w(z)$ raises this fraction to 98.9% and 99.97%, respectively.

In practice, it is also necessary to account for potential lateral misalignment of the beam with respect to the aperture axis (i.e., the nominal position of the transmitted beam), especially when considering the alignment of large-scale optical systems. Additionally, a Gaussian beam propagating through an aperture experiences diffraction losses, which affect its evolution: the beam waist decreases, potentially leading to mode mismatch.

The results presented in this paper are general and can be applied to various contexts and applications, among which their importance is fundamental in gravitational wave detectors.

2. Power Losses

The amount of power lost during the propagation of the Gaussian beam is referred to as power losses. In this paper, we focus on losses arising from clipping of the beam tails, as we are dealing with a Gaussian beam, which has an infinite intensity profile, and from lateral misalignment of the beam with respect to the aperture axis.

2.1. Clipping of the Gaussian Beam Tails

The transmitted power of a Gaussian beam propagating along the z-axis through a circular aperture is given by

$$P(r,z) = P_0\left[1 - e^{-\frac{2r^2}{w(z)^2}}\right] \tag{2}$$

where P_0 is the incident power, given by:

$$P_0 = \frac{1}{2}\pi w_0 I_0 \tag{3}$$

with w_0 and I_0 representing the incident beam waist and irradiance, respectively.

In the following, we will refer to an **aperture of radius** a. Fig. 1 shows the transmitted power as a function of the ratio $\frac{a}{w(z)}$, while Fig. 2 illustrates the associated power losses.

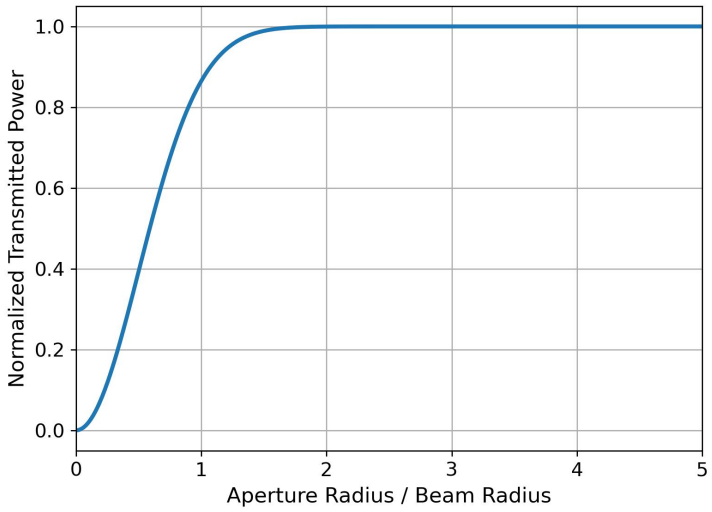

Fig. 1. *Normalized transmitted power of a Gaussian beam through a circular aperture, varying the aperture-to-beam size ratio from 0 to 5.*

The threshold loss for many experiments is approximately 1 ppm, which occurs when the ratio $\frac{a}{w(z)} > 2.6$, as shown in Fig. 3, and in Table 1.

2.2. Lateral Misalignment of the Gaussian Beam with Respect to the Aperture Axis

Another possible source of power loss is the misalignment of the beam with the aperture axis. The amount of misalignment depends on the parameters of the experiment. In this article, we consider the propagating beam with a lateral displacement up to 1.5 times its radius. Clearly, the value of the considered misalignment increases with the scale of the optical system under

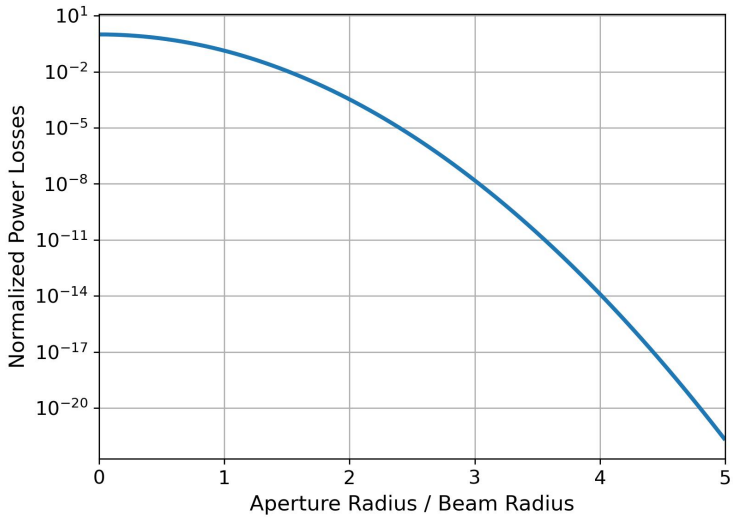

Fig. 2. *Normalized power losses of a Gaussian beam propagating through a circular aperture, as the aperture-to-beam size ratio is varied from 0 to 5.*

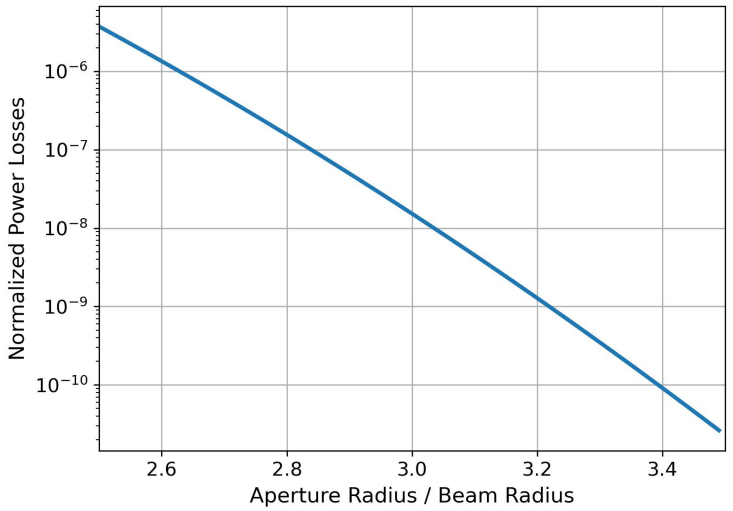

Fig. 3. *Normalized power losses of a Gaussian beam propagating through a circular aperture, zoomed for an aperture-to-beam size ratio varying from 2.5 to 4.5.*

a/w(z)	power losses (ppm)
2.50	3.73
2.75	2.70e-1
3.00	1.52e-02
3.25	6.69e-04
3.50	2.29e-05

Table 1. *Power losses due to clipping of the beam's tails for different aperture-to-beam size ratios.*

examination. For example, if we consider the design of dumping elements on optical benches where precise alignment is possible, we will have a lower misalignment threshold than the design of baffles within cavities tens or hundreds of kilometers long.
We consider a Gaussian beam propagating along the z-axis through a circular aperture of radius a, laterally displaced by a quantity d along the x-direction. We refer to the computation in [1]. The optical scheme illustrating this lateral shift is shown in Fig. 4.

The irradiance profile in Cartesian Coordinates (x', y', z), $I(x', y', z)$ is given by:

$$I(x', y', z) = I_{peak}\left(\frac{w_0}{w(z)}\right)^2 exp\left(-\frac{2((x')^2 + (y')^2)}{w(z)^2}\right) \tag{4}$$

where $z = z'$ since the aperture and the displaced beam have the same plane, I_{peak} is the peak irradiance of the Gaussian beam at the center of this position. If we consider a lateral displacement d along the x-axis, the irradiance can be written as:

$$I(x, y, z) = I_{peak}\left(\frac{w_0}{w(z)}\right)^2 exp\left(-\frac{2((x-d)^2 + (y)^2)}{w(z)^2}\right). \tag{5}$$

In cylindrical coordinates (r, θ, z), the equation 5 can be written as:

$$I(r, \theta, z) = I_{peak}\left(\frac{w_0}{w(z)}\right)^2 exp\left(-\frac{2r^2}{w(z)^2}\right) exp\left(-\frac{2d^2}{w(z)^2}\right) exp\left(\frac{4rd\cos\theta}{w(z)^2}\right). \tag{6}$$

Integrating the irradiance of the displaced beam from Eq. 6 over the entire aperture of radius a, we obtain the optical power P transmitted through a circular aperture (derived from the calculation in [1])

$$P = I_{peak}\left(\frac{w_0}{w(z)}\right)^2 exp\left(-\frac{2d^2}{w(z)^2}\right) 2\pi \sum_{k=0}^{\infty} \frac{4^k d^{2k}}{w(z)^{4k}(k!)^2} \times \left[a^{2k} 2^{-k-2} w(z)^2 \left(\frac{a^2}{w(z)^2}\right)^{-k} \left(\Gamma(k+1) - \Gamma\left(k+1, \frac{2a^2}{w(z)^2}\right)\right)\right] \tag{7}$$

where Γ is the gamma function, defined as:

$$\Gamma(s) = \int_0^{\infty} t^{s-1} e^{-t} dt. \tag{8}$$

The upper incomplete gamma function is defined as:

$$\Gamma(s,x) = \int_x^{\infty} t^{s-1} e^{-t}\, dt. \tag{9}$$

The lower incomplete gamma function is defined as:

$$\gamma(s,x) = \int_0^{x} t^{s-1} e^{-t}\, dt \tag{10}$$

which satisfy the following relation:

$$\gamma(s,x) + \Gamma(s,x) = \Gamma(s). \tag{11}$$

We can rewrite Eq. 7 using the lower incomplete gamma function as:

$$P = I_{peak}\left(\frac{w_0}{w(z)}\right)^2 exp\left(-\frac{2d^2}{w(z)^2}\right)2\pi \sum_{k=0}^{\infty} \frac{4^k d^{2k}}{w(z)^{4k}(k!)^2} \times \left[a^{2k}2^{-k-2}w(z)^2\left(\frac{a^2}{w(z)^2}\right)^{-k}\gamma\left(k+1, \frac{2a^2}{w(z)^2}\right)\right]. \tag{12}$$

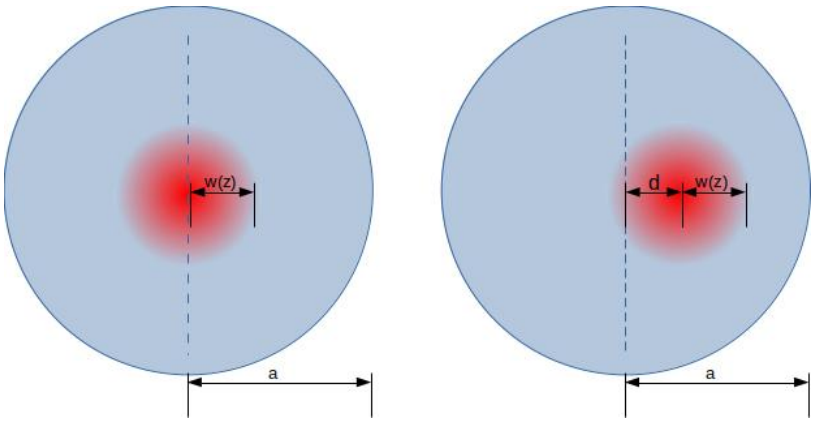

Fig. 4. *Gaussian beam propagating through a circular aperture. The solid circumference represents the circular aperture of radius a and the dashed circumference represents the section of the Gaussian beam at the aperture plane, whose radius is $w(z)$. On the left picture the beam is centered with the aperture, on right picture the beam is laterally displaced by a quantity d.*

From Fig. 5, we can observe different levels of power loss as a function of the ratio $a/w(z)$ and the variation of the lateral displacements. It is shown that to achieve losses of approximately 1 ppm with a displacement of $w(z)$, the aperture-to-beam radius ratio should be 3.5. On the other hand, for a displacement of 1.5 $w(z)$, the required ratio increases to 4.

3. Mode Mismatch Losses

In addition to power losses, we must also consider mode mismatch losses. They arise because the Gaussian beam is not perfectly matched to the fundamental TEM00 mode.
In the following, we will describe the mode mismatch due to the diffraction losses introduced by the circular aperture on the propagating beam.

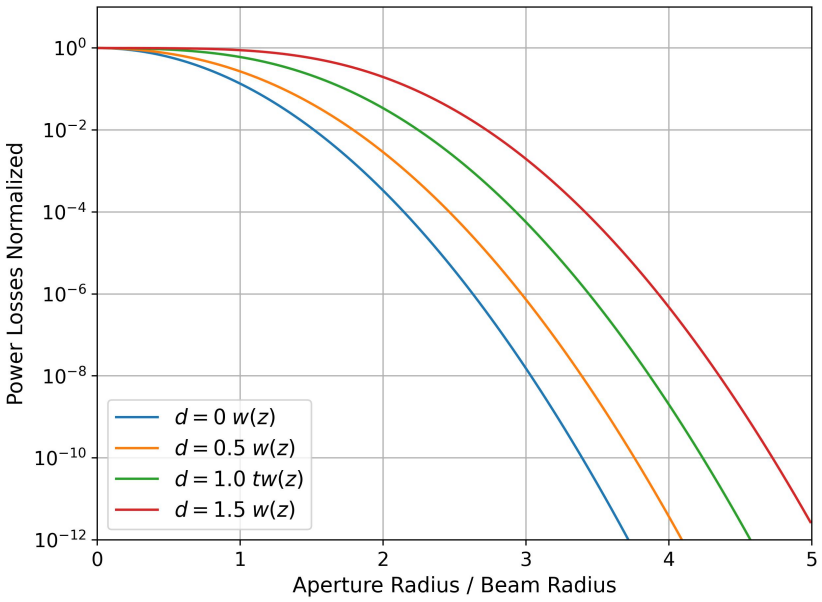

Fig. 5. *Power losses due to a laterally displaced beam, through a circular aperture of radius a, laterally displaced by* $d = 0, 0.5, 1.0, 1.5\ w(z)$.

3.1. Diffraction losses

A Gaussian beam can experience weak diffraction when passing through a circular aperture. Given the Gaussian nature of the beam, we adapt the ray optics diffraction formalism as detailed in [2]. The intensity of the wave along and in proximity of the propagation axis (z-axis), under near- and far-field approximations, is expressed as:

$$I(r,z) \sim \left(\frac{w_0}{w(z)}\right)^2 \cdot \left[1 - \delta_a e^{-i\pi F} J_0\left(\frac{2r\pi F}{a}\right)\right]^2. \tag{13}$$

Here, F represents the Fresnel number for a circular aperture, defined by $z/z_R = 1/\pi F$, where z_R is the Rayleigh range. J_0 denotes the Bessel function. We define $\delta_a = e^{-a^2/w_0^2}$, with $\delta_a \leq 1$. A value $\delta_a = 1$ corresponds to a uniform input of plane waves. The parameter δ_a distinguishes between near- and far-field approximations, roughly categorized as follows:

- $0.1 \leq \delta_a < 1$ indicates the near-field region;
- $\delta_a < 0.1$ indicates the far-field region.

For an aperture larger than 2.6 times the beam radius and $\delta_a < 10^{-3}$, we can consider the far-field approximation to be valid, so that the diffracted beam can be considered as a Gaussian beam [3]. We consider two different scenarios:

- The beam waist is on the aperture plane (Fig. 6);
- The beam waist is at a distance z from the aperture plane.

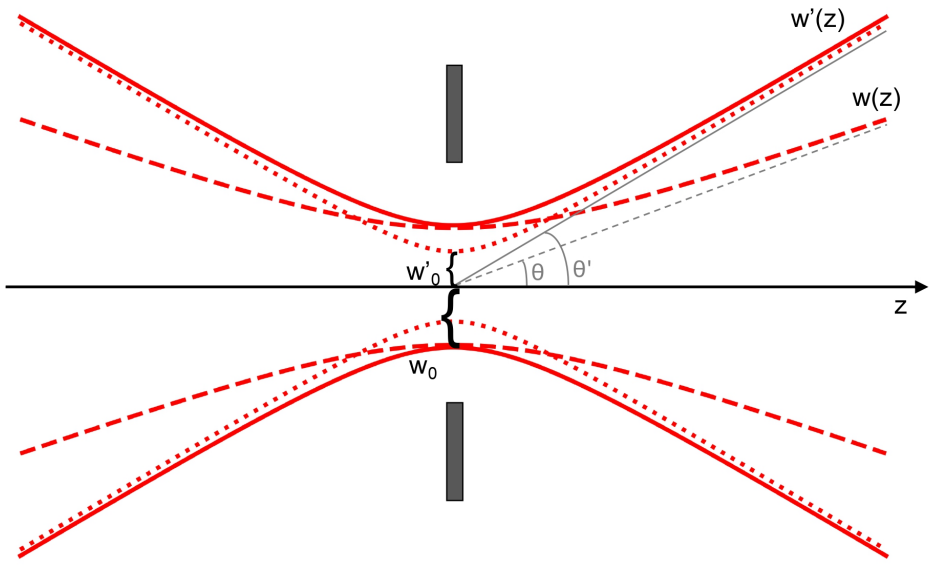

Fig. 6. *Changes in the Gaussian beam's profile while propagating through a circular aperture, when its waist is located on the aperture plane. The dashed line represents the incident beam without the diffraction introduced by the aperture. The solid line represents the beam diffracted by the circular aperture, whose waist coincides with the incident beam's and the divergence with the one of a dummy beam, whose waist is smaller (as shown by the dotted line).*

3.2. Beam Waist in the Aperture Plane

When the beam waist is located at the aperture plane ($w_0 = w(z)$), the ratio between the diffracted and incident waists is given by [3]:

$$1 - \frac{w_0'}{w_0} = 1 - \frac{w(z)'}{w(z)} \sim e^{-\frac{2a^2}{w(z)^2}}. \tag{14}$$

The difference between the two waists is less than 10^{-3} for the aperture-to-beam radius ratio considered ($a/w(z) > 2.5$).

3.3. Beam Waist along z

When the beam waist is not located on the aperture plane, the diffracted beam exhibits a different behavior. The ratio between the diffracted and incident waists (normalized to unity) is given by [3]:

$$1 - \frac{w_0'}{w_0} \sim e^{-\frac{2a^2}{w(z)^2}} \cos\left(p \frac{a^2}{2\pi w(z)^2}\right) \tag{15}$$

where $p = \sqrt{2}z\lambda/w_0^2$, where λ is the wavelength of the laser.

In Fig. 8, we present different curves corresponding to various values of the parameter p, considering $p = 0, 1, 5, 7, 10$. The difference in waist size between incident and diffracted beams is small for $a/w(z) > 2.8$, where the contribution of the cosine term begins to be negligible.

Through this initial analysis, we have determined how the beam waist changes due to diffraction by a circular aperture. The associated mode mismatch is then derived by evaluating the overlap integral between the input beam and the diffracted beam.

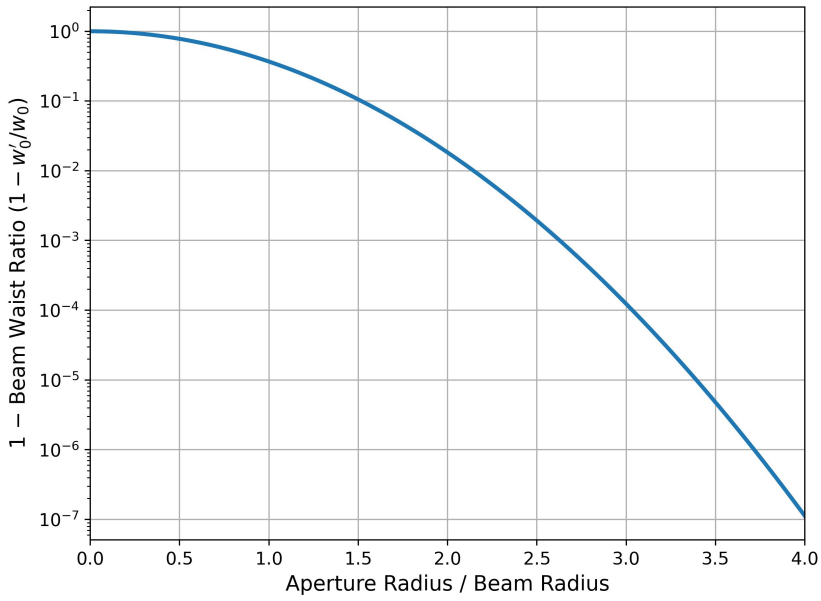

Fig. 7. *Relative difference between the waists of the diffracted and incident beams as a function of the aperture radius-to-beam size ratio.*

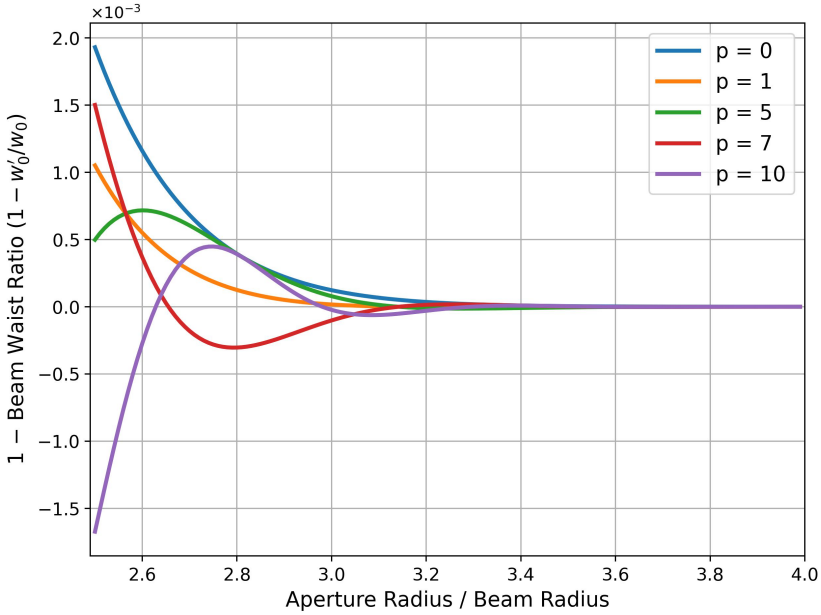

Fig. 8. *Difference between the diffracted and incident beams as a function of the aperture radius-to-beam size ratio, for different values of the parameter p.*

3.4. Mode Mismatch using Overlap Integral

Mode matching arising from Gaussian beam diffraction can be quantified using an overlap integral between the input beam and the diffracted beam. The coupling efficiency of optical power can be computed as the square of this overlap integral, using the following formula:

$$\eta = \frac{\left| \int E_1^* E_2 dA \right|^2}{\int |E_1|^2 dA \int |E_2|^2 dA} \tag{16}$$

where E_1 and E_2 are the complex electric fields of the two beams in a plane.

We computed the Overlap Integral (OI) between the transmitted beam and the beam weakly diffracted by the circular aperture of radius a, using OSCAR (Optical Simulation Containing Ansys Results) [4], a Matlab-based FFT code.
The waist of the diffracted beam, from Eq 15, is:

$$w_0' = 1 - w_0 \left[e^{-\frac{2a^2}{w(z)^2}} \cos\left(p \frac{a^2}{2\pi w(z)^2} \right) \right] \tag{17}$$

where we recall that $p = \sqrt{2} z\lambda / w_0^2$, w_0 is the waist of the input beam , a is the aperture radius, $w(z)$ is the beam radius at the aperture plane, z is the distance between the aperture and the beam waist.
In this analysis, it is possible to consider the astigmatism of the beam, considering different beam sizes in the tangential and sagittal planes. In Fig. 9, we show the mode mismatch (MM), calculated as MM = 1 - OI, as a function of the ratio $a/w(z)$. We observe that the mode mismatch is well below 1%, which is a common threshold in many experiments, for a ratio $a/w(z)$ between 2.5 and 4.

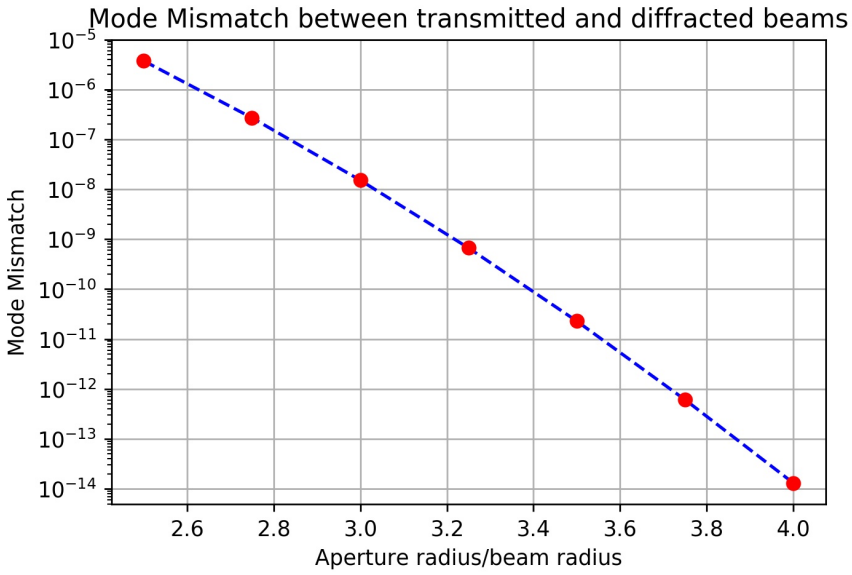

Fig. 9. *Mode mismatch as a function of aperture radius over beam size in the case of $p < 10^{-3}$, so close to the case of beam waist at the aperture plane.*

4. Application in Gravitational Waves Detectors

Among various applications, this study is helpful in the design of several components for ground-based gravitational wave detectors, LIGO in the United States [5], and Virgo in Europe [6]. Given the requirements on optical losses and mode mismatch on the propagating Gaussian beam, one can dimension the size of mirrors, vacuum tubes, and apertures of dumping objects (diaphragms and baffles). The last application is what motivated this study. In particular, a gravitational wave detector system particularly sensitive to optical losses and mode mismatch is the squeezing system that uses vacuum squeezed states to reduce quantum noise in interferometers [7]. This technique has been implemented by both Virgo [8] and LIGO [9] for the O3 observing run starting in 2019, introducing frequency-independent vacuum squeezed states. Subsequently, significant infrastructural and optical modifications were made to the squeezing system to achieve broadband quantum noise reduction in preparation for the O4 observing run, producing frequency-dependent squeezing by reflecting squeezed states by a suspended cavity, called filter cavity [10, 11]. In this case, the squeezed states propagate through a large-scale system, covering optical paths ranging from tens to hundreds of meters, as shown in Fig. 10 for the system in Virgo. The vacuum squeezed states are generated and then travel across two suspended benches linked by a 12-meter tube before reaching the 285-meter-long cavity after passing through a 40-meter tube. Therefore, it is necessary to account for the jitter carried by the beam arriving at the input mirror of the filter cavity. To keep the beam aligned in such an extended system, two feedback control loops operate simultaneously. These loops are implemented on a green beam propagating through the system, which overlaps with the infrared field of the squeezing. Therefore, in this analysis, we assume perfect beam overlap. The first loop is a wavefront sensing loop, also known as the Automatic Alignment (AA) loop, which is implemented in the filter cavity to maintain alignment between the beam axis and the cavity axis. It uses quadrant photodiodes in reflection from the filter cavity and acts on the suspended cavity mirrors to minimize the first misalignment mode, namely TEM10 or TEM01. It is necessary to keep the beam centered on the cavity mirrors, which is not always possible because of drifts and jitters due to temperature, mechanical settlements and tides. For this purpose, a second beam pointing control (BPC) loop is used. Dither lines are applied to the suspended mirrors of the filter cavity and subsequently demodulated to generate the error signal. The actuation takes place on mirrors located tens of meters away from the cavity in reflection. The relative drift of these control loops is measured by beam position sensors on the mirrors and corresponds to 0.12 mm in the horizontal direction and 0.02 mm in the vertical direction on the input mirror. The residual beam jitter is orders of magnitude smaller than the 2 cm diameter of the infrared beam on the mirrors. However, it has been shown that the beam must be decentered on the mirrors to avoid point absorbers and therefore excessive cavity losses [12]. The area considered on each cavity mirror is 1.7 cm, which is comparable to the diameter of the beam. This means that when designing diaphragms on the benches or baffles inside the tubes, a lateral misalignment of at least $w(z)$ must be taken into account. These considerations have been taken into account for the design of diaphragms and baffles to be installed in Virgo to block stray light. In particular, a lateral misalignment of one beam radius has been considered on the benches, where it is on the order of millimeters, and 1.5 times the beam radius within the 40-meter tube and the cavity, where it is on the order of centimeters. It should be noted that the optical path in the cavity must be doubled, as losses are considered in terms of round-trip losses [13]. For power losses, the requirement is to be of the same order of magnitude of the losses due to the imperfection of highly reflective mirror coatings, around 1 ppm. This value is one order of magnitude lower than the expected round-trip losses inside the 285 meters cavity. For mode mismatch, the requirement on the squeezing system is 1%. Therefore, the aperture can introduce a mode mismatch of one order of magnitude below, i.e. 0.1% [10].

In this specific system, we can conclude that to achieve optical losses below 1 ppm, considering a lateral displacement of 1 - 1.5 w(z), the aperture-to-beam radius ratio ($a/w(z)$) should be

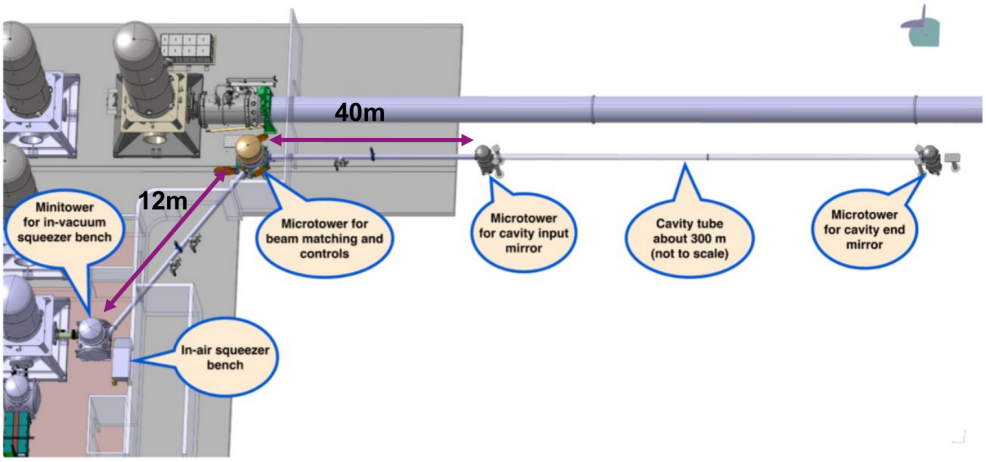

Fig. 10. *Experimental setup of frequency-dependent squeezing system in Virgo. The in-air bench sends the beam to a suspended bench connected to a second one by a 12-meters tube. The beam is then sent to the 285-meters filter cavity through a 40-meters tube.*

chosen as 3.5 for diaphragms and 4.0 for baffles. Since the global mode mismatch requirement for is 1%, and individual contributions are considered at 0.1%, we can conclude that the diffraction effect is negligible in this case.

Conclusions

We have examined the loss mechanisms affecting a Gaussian beam propagating through a circular aperture. We considered optical losses due to beam tail clipping and lateral misalignment, as well as mode mismatch losses arising from beam diffraction at the aperture. The computations and degradation mechanisms discussed in this paper can be applied in various contexts. Indeed, considering different loss thresholds, we have different aperture-to-beam size ratios. As a specific example, we applied these findings to determine the aperture sizes of diaphragms and baffles in the context of large-scale optical systems such as gravitational wave detectors.

5. Acknowledgement

The authors thank the Quantum Noise Reduction team of Advanced Virgo for the useful discussions during the working group meetings. In addition, a further acknowledgment goes to M. Vardaro and Y. Zhao for useful discussions during the writing of the manuscript.

References

1. T. S. Khwaja and S. A. Reza, "Low-cost gaussian beam profiling with circular irises and apertures," Appl. optics **58**, 1048–1056 (2019).
2. A. E. Siegman, "Lasers university science books," Mill Val. CA **37**, 169 (1986).
3. P. Belland and J. P. Crenn, "Changes in the characteristics of a gaussian beam weakly diffracted by a circular aperture," Appl. Opt. **21**, 522–527 (1982).
4. J. Degallaix, "Oscar a matlab based optical fft code," in *Journal of Physics: Conference Series,* vol. 228 (IOP Publishing, 2010), p. 012021.
5. T. L. S. Collaboration, J. Aasi, B. Abbott, *et al.*, "Advanced ligo," Class. Quantum Gravity **32**, 074001 (2015).
6. F. Acernese, M. Agathos, K. Agatsuma, *et al.*, "Advanced virgo: a second-generation interferometric gravitational wave detector," Class. Quantum Gravity **32**, 024001 (2014).
7. C. M. Caves, "Quantum-mechanical noise in an interferometer," Phys. Rev. D **23**, 1693 (1981).

8. F. Acernese *et al.*, "Increasing the astrophysical reach of the advanced virgo detector via the application of squeezed vacuum states of light," Phys. Rev. Lett. **123**, 231108 (2019).
9. M. Tse *et al.*, "Quantum-enhanced advanced ligo detectors in the era of gravitational-wave astronomy," Phys. Rev. Lett. **123**, 231107 (2019).
10. F. Acernese *et al.*, "Frequency-dependent squeezed vacuum source for the advanced virgo gravitational-wave detector," Phys. Rev. Lett. **131**, 041403 (2023).
11. D. Ganapathy *et al.*, "Broadband quantum enhancement of the ligo detectors with frequency-dependent squeezing," Phys. Rev. X **13**, 041021 (2023).
12. Y. Zhao, M. Vardaro, E. Capocasa, *et al.*, "Optical losses as a function of beam position on the mirrors in a 285-m suspended fabry-perot cavity," Phys. Rev. Appl. **22**, 054040 (2024).
13. N. Hodgson and H. Weber, *Laser Resonators and Beam Propagation: Fundamentals, Advanced Concepts, Applications*, vol. 108 (Springer, 2005).